Cellular and Molecular Biology

Journal homepage: www.cellmolbiol.org

The prognostic value of N6-methyladenosine RBM15 regulators in lung adenocarcinoma

Mingsheng Ma[1,2], Wei Wang[3], Biying Wang[1], Yichen Yang[1], Yunchao Huang[1], Guangqiang Zhao[1], Lianhua Ye[1*]

[1]*Department of Thoracic Surgery, The Third Affiliated Hospital of Kunming Medical University, Kunming, Yunnan,650118, China.*
[2]*Department of Cardiothoracic Surgery, The Sixth Affiliated Hospital of Kunming Medical University, Yuxi,Yunnan,653100, China*
[3]*Department of Thoracic Surgery, Taihe Hospital (Hubei University of Medicine), Shiyan, Hubei,442000, China*

ARTICLE INFO

Original paper

Article history:
Received: July 08, 2021
Accepted: January 20, 2022
Published: January 30, 2022

Keywords:
RBM15; Lung adenocarcinoma; m6A demethylase; siRNA; Mechanisms; Cellular functions

ABSTRACT

N6-methyladenosine (m6A) is the most common internal modification in mammalian mRNAs while RNA-binding motif protein 15 (RBM15) is an important methyltransferase in m6A modification. Increasing evidences have shown that RBM15 has a close correlation with lung cancer. However, specific functions of RBM15 in lung adenocarcinoma (LUAD) are limited. RBM15 expression was analyzed in human LUAD tissues and matched healthy lung tissue. RBM15 was knocked down via siRNA in A549 and H1734 cells. The relationships between RBM15 with cellular functions characteristics and mRNA m6A levels were explored. We performed functional characterization in A549 and H1734 cells lines to elucidate the molecular role of RBM15. Results found that RBM15 was up-regulated in the LUAD tissue and cells, which was linked to poor survival of LUAD patients. RBM15 can be knocked down via siRNA in A549, which leads to the exploration of the associations between RBM15 with cell characteristics. In vivo, RBM15 knockdown could decrease the methylation level, reduce proliferation, accelerate apoptosis and inhibit tumor growth. Our research shows that RBM15 facilitates LUAC cell progression by m6A demethylation. However, it is necessary to conduct further researches on potential downstream molecular mechanisms and m6A modification of RBM15 activity in LUAC.

DOI: http://dx.doi.org/10.14715/cmb/2022.68.1.17

Introduction

Lung cancer is the most remarkable death-related malignant tumor in worldwide (1-4). In the USA, about 220,000 lung cancer cases were newly diagnosed and more than 140,000 deaths were reported in 2019(5). Non-small cell lung cancer (NSCLC) is the most prevalent type of lung cancer, including lung adenocarcinoma (LUAD), which is the most common subtype in non-small cell lung cancer and is attributed to smoking (6-9) with very short survival time, and lung squamous cell carcinoma. Although the methods for diagnosing lung adenocarcinoma and the treatments for it have been developed over the past few decades, the average survival rate of patients with lung cancer is less than 20% within 5 years. Therefore, it is of vital importance to explore effective methods for early diagnoses by further studying the molecular mechanism of LUAD to enhance the therapeutic effect, thus improving the LUAD patients' quality of life.

N6-methyladenosine (m6A) modification is one of the most abundant and reversible internal modifications in eukaryotes and mammalian cells (10). RNA m6A modification was first described in the 1970s without gaining any special attention. In recent years, m6A modification has obtained a renewed interest in cancer or non-cancer research as a new layer of control for gene expression (11). More and more evidences demonstrated the vital roles of epigenetics modification for cancer as well as m6A, such as microRNA (12, 13), noncoding RNA, chromatin remodeling and histone modification (14-19). It has been indicated that m6A mRNA methylation modification is regulated by three major functional enzymes, including methyltransferase (METTL3, METTL14, WTAP, RBM15) (20), demethylase (ALKBH5, FTO) (21), and methylated reader proteins (YTHDF1/2/3, HNRNPA2B1, IGF2BP) (22). m6A influences mRNA structure, stability and maturation, thus playing multiple roles in modulating biological processes.

RNA-binding motif protein 15 (RBM15) is a subgroup of the N6-adenosine methyltransferase family. Several recent reports have demonstrated aberrant m6A modification to have exerted critical

*Corresponding author. E-mail: lhye1204@aliyun.com

roles on lung cancer development. High RBM15 expression is found to be associated with a variety of cancers, including ovarian cancer and cervical squamous cell carcinoma（CESC）(23, 24), while limited researches were carried out on the relationship between RBM15 and lung adenocarcinoma.

In this research, the prognostic role of RBM15 in LUAC was evaluated. The relationship between RBM15 expression and the LUAC survival rate was analyzed by the Cancer Genome Atlas (TCGA) database. A biological function experiment was performed to explore the function of RBM15 in A549 and H1734 cells. Finally, RBM15 was found to have been up-regulated in the LUAD tissue and cells, and have installed the N6-methyladenosine modification, thereby regulating the proliferation and apoptosis of LUAD.

Materials and methods

Publicly available gene expression data sets

RBM15 gene expression levels were analyzed by the TCGA database. To explore the potential roles of RBM15 in LUAD, the relationships between RBM15 expression levels and the LUAD survival proportions were analyzed by the Kaplan-Meier plotter database (http://kmplot.com/analy sis/), with all the data directly achieved online.

Clinical samples

The study was approved by the Ethical Committee of the Third Affiliated Tumor Hospital of Kunming Medical University, where the paraffin-embedded specimens and negative 80 degrees from 40 LUAC tissues and corresponding normal tissues were collected from March 2019 and January2021.

Immunohistochemistry

Paraffin-embedded sections (4 μm thick) were done for staining on polylysine-coated slides. 10mmol/L sodium citrate (pH 6.0) was used to achieve antigen retrieval. In addition, 10% of normal goats were raised for blocking serum, and then rabbit monoclonal antibodies were incubated to resist RBM15 (EPR6895, Abcam, 1:1000) overnight at 4 °C. Then, with secondary antibody (Vector Laboratories) incubated, DAB Substrate Kit was used for staining using Peroxidase. RBM15 expression was analyzed based on the number of positive cells and the staining intensity. ACARL-ZEISS observer A1 camera and ZEN 2.3 Camedia software were used to acquire the images. All cases about the study and the images were quantified on Image Pro by two pathologists.

Cell culture

The Beas-2B, A549, H1734, H838, SPC-A1, H1299 human LUAC cell lines were obtained from the Kunming Institute of Zoology, Chinese Academy of Sciences (Kunming, People's Republic of China) in October 2019. The cells were cultured in 1640 and DMEM medium (Sigma, St. Louis, MO, USA) with 10% fetal bovine serum (FBS) (Gibco, NY, USA) cultured in 5% CO2 cell culture at a temperature under 37 °C.

Plasmid construction and transfection

RBM15 small interfering RNA (siRNA) and negative control siRNA plasmids were obtained from VectorBuilder (Guangzhou, China). Transfection was performed in A549 cells and H1734 cells by using Lipofectamine 2000 (Invitrogen, Carlsbad, CA). The medium was replaced with a fresh medium 12 h after transfection.

Total RNA preparation, cDNA synthesis, and quantitative reverse transcription PCR (qRT-PCR)

RBM15 total RNA was drawn with E.Z.N.A.TM Total RNA Kit I (Omega). For cDNA synthesis, 2000 ng of total RNA was applied in reverse transcription of a 10 μL reaction volume with a PrimeScript™ RT reagent kit (TaKaRa) under the manufacturer's instructions. Then, Qrtpcr was used with TB Green™ Premix Ex Taq™ II (TaKaRa) in a Roche LightCycler®96qRT-PCR system. With GAPDH serving as endogenous control, each response was run in triplicate. The qRT-PCR primers used are listed in Table 1.

Table 1. The list of qRT-PCR primers used

Primer	Forward	Reverse
RBM15	CTCCGACGACCCG	CCACCAGAGCCCCCTAA
Gapdh	CAACAAT	CTT
	CGCTGAGTACGTC	GCTGATGATCTTGAGGC
	GTGGAGTC	TGTTGTC

Western blot analysis

Total protein components of cells or tumor tissues were extracted with RIPA lysis buffer (50 mMTris-HCl, 100 mM NaCl, pH 7.5, Triton, EDTA, and glycerophosphate) in the presence of protease inhibitor. The concentration was measured by using a BCA protein kit (Pierce, USA). Then, cell extractions were separated by using 12% SDS-PAGE and subsequently transferred onto polyvinylidene difluoride (PVDF) membranes (Amersham Pharmacia, Germany). The membranes were incubated with primary antibodies (anti-RBM15, Abcam, ab96544) at 4 °C overnight, followed by the enhanced chemiluminescence (ECL, Amersham Pharmacia, USA) with goat anti-rabbit GAPDH (Sigma, USA) for 1 h at room temperature.

Cell proliferation assay

Cell proliferation was estimated by using Cell Counting Kit-8 (CCK-8; Dojindo Laboratories) under the manufacturer's instructions. The cells were seeded on a 96- well plate at a density of 2000 cells/100 μL. Subsequently, 10% of total volume CCK-8 solution was added according to the indicated different time points. After incubation at 37 °C for 8 h, the absorbance at 450 nm was checked on a microplate reader (Thermo Varioskan™ LUX). The experiment was conducted in triplicates.

Migration assay

Cells were seeded in six-well plates for 24 h until attach-wall and then scratched. Photomicrographs were acquired at different time points. Finally, the wound-healing ratio was measured using Image J.

Colony formation assay

500 cells were seeded in six-well plates for the colony-formation assay. Formed colony balls were calculated after two-three weeks.

Cell invasion and migration assay

For the invasion assay, 3×10^4 cells were resuspended and then seeded into the upper chamber of a Transwell in a serum-free medium, with 20% serum medium added to the bottom chamber. For the migration assay, 1×10^5 cells were resuspended and then seeded into the upper chamber of a Transwell in serum-free medium, with 20% serum medium added to the bottom chamber. A thin layer of Matrigel was used for the separation from the upper chamber by a membrane with an 8 μm pore size coating. After 24 h and 48 h, invaded and migrated cells were fixed with methanol and then stained with 1% crystal violet for cell counting respectively.

Cell cycle and apoptosis assay

The cells of each group were collected and fixed overnight in 70% ethanol at 4℃ and stained with 25μg/ml PI containing 1μg/ml RNase at 37℃. Cell cycle distribution ratio in different intervention groups was detected with flow cytometric analysis. Cells were harvested and then re-suspended, with 5 μL of 7-AAD and 5 μL of PE Annexin V added to the cell suspension (BD, USA). After staining for 30 min, the cells were used for flow cytometric analysis.

Measurement of the m6A total RNA level

Total RNA was extracted from tissues and cells by using TRIzol Reagent （15596018，Life Technologies，USA. To detect the relative content of m6A in the total RNA, an EpiQuik™ m6A RNA Methylation Quantification Kit (P-9005，EpiGentek, USA)was used under the manufacturer's instructions. In brief, 200ng of RNA was allocated in each well, with the addition of the solution containing the antibodies. The m6A levels were then measured colorimetrically by setting the absorbance at 450 nm on an automatic microplate reader (BioTek ELx800, USA).

Dot plot assay

Total RNA was extracted from tissues and cells by using TRIzol Reagent （15596018, Life Technologies, USA. The concentration of the RNA was measured and diluted to 0.33ug/μl, with 1 μl of each sample loaded to an Hybond-N+ membrane (GE Healthcare) and crosslinked by 254 nm ultraviolet ray for 5 min by using Spectroline XL-1000 (Spectroline, New York City, NY, USA). After PBS flushing, membranes were stained with 0.02% methylene blue (Sangon Biotech) for 5 min and blocked with 5% BSA (A8020, Solarbio, China). Primary m6A antibodies (1:1000, ab208577, Abcam, UK) were used for incubation overnight at 4 °C, and anti-mouse IgG (1: 5000, Beyotime Biotechnology) was incubated at

room temperature for 1 h. Images were acquired through the QuickChemi5100 Chemiluminescence system (Monad, China) and analyzed by Image J (National Institutes of Health, Bethesda, MD, USA).

Statistical analysis

With the data demonstrated as the means ± standard deviations, statistical analyses were conducted on SPSS 22.0, showing the graphical representations on Graph Pad Prism 5. The Student's t-test was adopted to analyze the significance of differences between different groups, whereas one-way analysis of variance was carried out to make comparisons among more than one group, with P values less than 0.05 from different groups considered statistically significant.

Results and discussion

RBM15 expression is correlated with human lung cancer

Data from TCGA database demonstrated that RBM15 expression was higher in LUAD tissues than that in normal tissues, suggesting RBM15 to be participating in lung cancer formation and RBM15 up-regulation to be significantly correlated with a low LUAD survival rate (Fig.1A). Immunohistochemistry staining was carried out to observe RBM15 expression in 40 cases of LUAD tissues and the normal tissue controls, leading to the results that RBM15 protein significantly increased in LUAD tissues, and RBM15 was mainly expressed in the cytoplasm (Fig.1B). Western blot analysis indicated that RBM15 proteins were expressed high in the LUAD cancer tissues (Fig.1C), while RT-PCR analysis demonstrated that RBM15 mRNA was expressed high in the LUAD cancer tissues (Fig.1D).

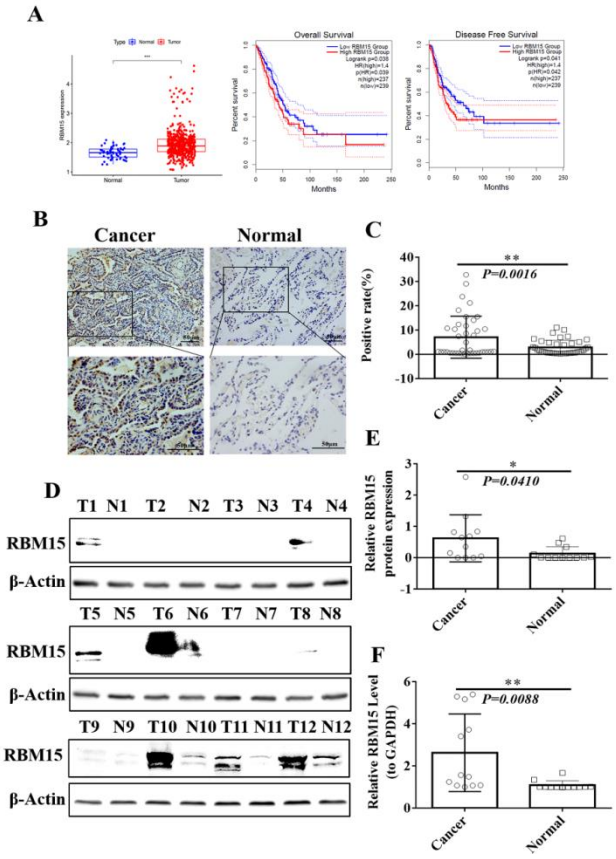

Figure 1. RBM15 expression correlates with human lung cancer. (A) The levels of RBM15 expression in LUAD (n=535) and normal tissues (n=59) were analysed by TCGA data. Kaplan-Meier survival curves of OS and DFS based on RBM15 expression using the online bioinformatics tool Kaplan-Meier Plotter. (B) The RBM15 protein was expressed in LUAD tissues and normal lung tissues by immunohistochemistry staining(n=40). (C)Bar graphs showing the Positive rate quantitative analysis results.(D) The protein level of RBM15 in LUAD tissues and normal tissues by Western blot analysis(n=12).(E) Bar graphs showing the Western blot quantitative analysis results.(F) The mRNA level of RBM15 in LUAD tissues and normal tissues by RT-PCR analysis(n=12).Bar graphs: mean ± SD. *P<0.05,**P<0.01.

RBM15 expression in different LUAD cells

Western blot and RT-PCR analysis were conducted to observe RBM15 protein and mRNA expression in 5 cases of LUAD cells and the control of normal alveolar epithelium cells, leading to the result that the RBM15 protein and mRNA expression were significantly high compared with normal alveolar epithelium cells (Fig.2A-C).

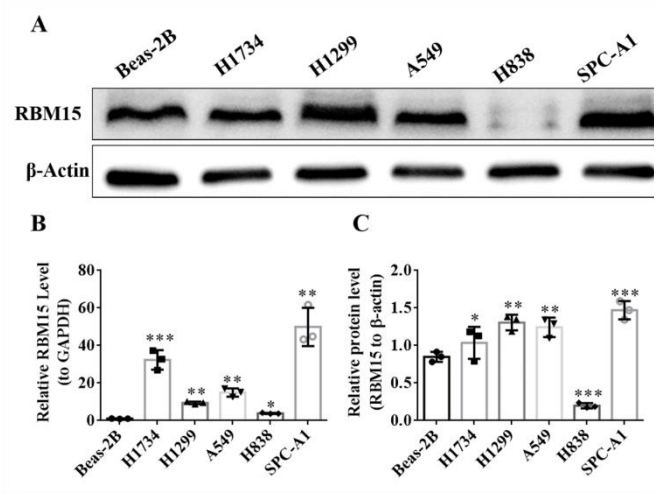

Figure 2. RBM15 expression correlates with different LUAD Cells. (A) The protein level of RBM15 in different LUAD cells by Western blot analysis. (B) The mRNA level of RBM15 in different LUAD cells by RT-PCR analysis. (C) Bar graphs showing the Western blot quantitative analysis results. Bar graphs: mean ± SD. *P<0.05, **P<0.01, ***P<0.001.

Silencing of RBM15 represses the expression of RBM15 protein in A549 and H1734 cells

The silencing of RNA (siRNA) targeting the RBM15 was transfected into A549 and H1734 cells to silence the RBM15 expression. Western blot analysis indicated that the RBM15 protein level decreased after the transfection, withsiRBM15-2 significantly reducing the levels of RBM15 protein (Fig.3A-B), and that RT-PCR siRBM15-2 mRNA had remarkably reduced the levels of RBM15 mRNA (Fig.3C-D).

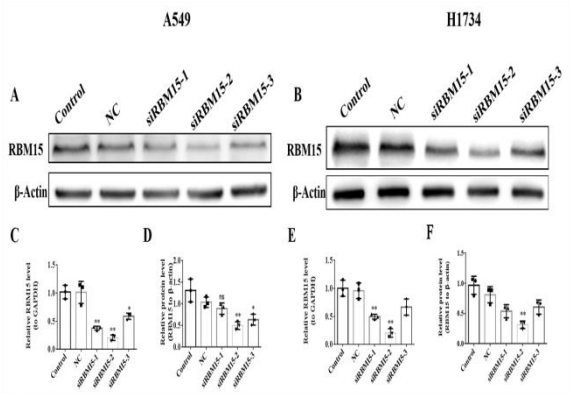

Figure 3. Silencing of RBM15 represses the expression of RBM15 protein in A549 and H1734 cells. The silencing of RNA (siRNA) targeting the RBM15 transfected into A549 and H1734 to silence the RBM15 expression. （A-B）Western blot analysis indicates the RBM15 protein level.(C-D) RT-PCR analysis indicated the RBM15 mRNA level. (E-F) Bar graphs showing the Western blot quantitative analysis results. Bar graphs: mean ± SD. *P < 0.05, **P < 0.01.

RBM15 knockdown inhibited LUAD cell proliferation activity

To examine the roles of RBM15 in LUAD, RBM15 was knocked down in A549 and H1734 cells. RBM15knockdownsignificantly inhibited A549 and H1734 cell proliferation (Fig.4A-B). Flow cytometry data showed knockdown of RBM15to have increased the apoptosis rate in A549 and H1734 cells (Fig.4C-D), while flow cytometry data demonstrated that knockdown of RBM15 had increased the ratio of G0/G1 phase cells, and reduced the ratio of S, G2/M phase cells (Fig.4E-F), suggesting that RBM15 plays a vital role in LUAD cell proliferation.

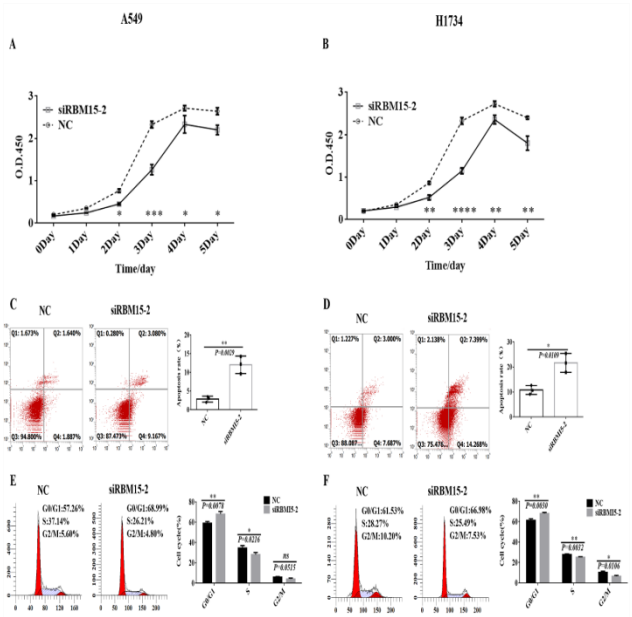

Figure 4. RBM15 regulates LUAD cell characteristics. (A-B) RBM15 influenced LUAD cell proliferation in A549 and H1299 cells. Cell proliferation was assessed by Cell Counting Kit-8 assay. RBM15 influenced the following cell growth characteristics of A549 and H1299 cells: (C-B) apoptosis, (E-F) cell cycle. Bar graphs: mean ± SD. *P < 0.05, **P < 0.01, ***P < 0.001. Bar graphs: mean ± SD. *P<0.05, **P<0.01, ***P<0.001,****P<0.0001.

RBM15 knockdown repressed colony formation, migration, and invasion

To examine the roles of RBM15 in LUAD, RBM15 was knocked down in A549 and H1734 cells, with the successful RBM15 knockdown confirmed at the mRNA and protein levels (Fig.3A-D). RBM15 knockdown significantly repressed the ability of A549 and H1734 cells to form colonies (Fig.5A-B). The results of Transwell migration and invasion assays also showed that there were significantly less invasive cells

in the RBM15 group than those in the control group (Fig.5C-F). Furthermore, the findings of the invasion assay indicated that RBM15 had reduced the invasion of cells into the blank scratched area compared with that in the control group (Fig.5G-I). As expected, RBM15 knockdown had suppressed cell colony formation, invasion and migration (Fig.5A–I). Altogether, these results suggest that RBM15 plays a vital role in LUAD cell proliferation, metastasis, and invasion.

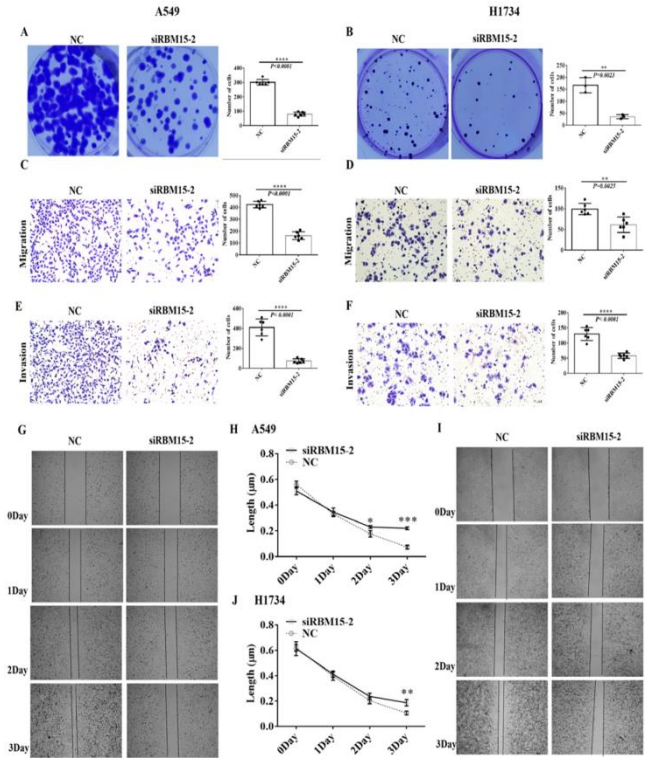

Figure 5. RBM15 regulates LUAD cell characteristics. Cell proliferation was assessed by Cell Counting Kit-8 assay. RBM15 influenced the following cell growth characteristics of A549 and H1734 cells: (A-B) colony formation ability, (C-D) migration, (E-F) invasion, (G-I) Cell proliferation was assessed by Cell Counting Kit-8 assay. Bar graphs: mean ± SD. *P<0.05, **P < 0.01, ***P < 0.001,****P<0.0001.

RBM15 regulates mRNA m6A levels of LUAC tissues and cells

To further detect the underlying mechanisms of RBM15 in LUAC, m6A levels of the LUAD tissues and normal tissues from 12 cases detected by the dot plot assay experiment and colorimetric ELISA-like assay. Compared with those in normal tissues, m6A levels in LUAD tissues had significantly increased (Fig.6A). The colorimetric ELISA-like assay and dot plot assay experiment were conducted to observe RBM15 m6A levels in the LUAD cells of 5 cases and the normal alveolar epithelium cells control, leading to the result thatm6A levels of the RBM15 expression were significantly high compared with those of the normal alveolar epithelium cells (Fig.6B).M6A levels of A549 cells had been decreased by the silencing of RBM15 in the dot plot assay experiment and colorimetric ELISA-like assay compared with those in the control group(Fig.6C). Dot plot assay experiment and colorimetric ELISA-like assay demonstrated that m6A levels of H1734 cells were obviously decreased silencing of RBM15 came into play (Fig.6D). Therefore, RBM15 plays a role in regulating the m6A modification in LUAC tissues.

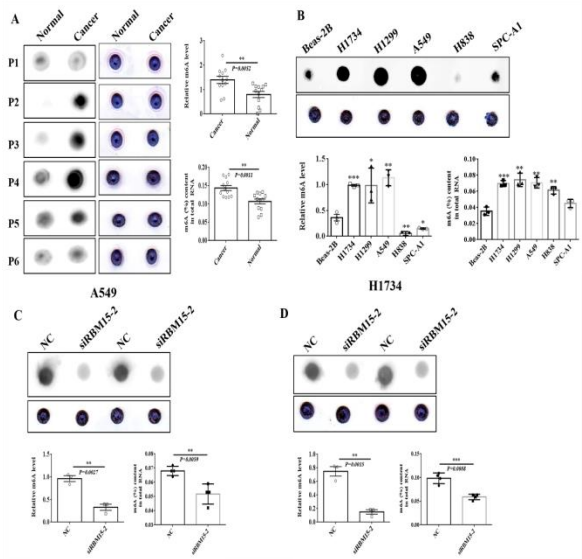

Figure 6. RBM15 regulates LUAD tissues and cellm6A levels by the dot plot assay experimental and colorimetric ELISA-like assay.

(A) The mRNAs isolated from LUAD tissues and paired normal tissues were used in dot blot analyses with an anti-m6A antibody, with methylene blue staining serving as the loading control. The relative m6 A level on mRNA in LUAD tissues and paired normal tissues were calculated (right panel, n=12). The m6A content in total RNA from the same 12 LUAD tissues and paired normal tissues were detected by colorimetric ELISA-like assay via the m6 A RNA methylation quantification kit.(B) The relative m6A level and the m6A content in total RNA in 5 cases of LUAD cells and matched normal alveolar epithelium cells using dot plot assay experiment and colorimetric ELISA-like assay. (C-D) When dealing with A549 and H1734 cells by the silencing of RBM15. ThemRNAs isolated from A549,H1734 cells and paired numerical

control were used in dot blot analyses with an anti-m6A antibody, with methylene blue staining serving as the loading control. The relative m6A level on mRNA in A549, H1734 cells and paired numerical control were calculated. The m6A content in total RNA n A549, H1734 cells and paired normal tissues were detected by colorimetric ELISA-like assay via the m6 A RNA methylation quantification kit. Bar graphs: mean ± SD.*P<0.05, **P < 0.01, ***P < 0.001.

The association of RBM15 expression with clinicopathological features

The study was approved by the Ethical Committee of the Third Affiliated Tumor Hospital of Kunming Medical University, where the paraffin-embedded specimens and negative 80 degree from 40 LUAC tissues and corresponding normal tissues were collected from March 2019 and January2021. The study was carried out to find whether RBM15 expression level is associated with the clinicopathological features of gender, age(yr), tumor location, tumor size(cm), tumor stage (T stage), lymph node metastasis（LN stage）, TNM stage (tumor, node, metastasis stage), histopathological typing in LUAD. Immunohistochemistry was also conducted to observe RBM15 expressions in these 40 cases of LUAD tissues and control normal tissues (Fig.1B), revealing that RBM15 expressions are associated with LN metastasis (lymph node metastasis), TNM stage (tumor, node, metastasis stage) and histopathological typing (Table 2).

Table 2. Relationship between RBM15 expressions and clinicopathological parameters in lung adenocarcinoma

Variables	Patients number	RBM15 expression in tumor tissue	P value
Gender	40		0.5030
Male	14	8.308 ± 7.624	
Female	26	6.359 ± 9.204	
Age(yr)	40		0.9676
≥60	15	6.968 ± 8.824	
<60	25	7.085 ± 8.703	
Whether smoking	40		0.3484
Yes	13	8.911 ± 7.580	
No	27	6.140 ± 9.096	
Tumor location	40		0.2557
Upper lobe of left lung	10	4.194 ± 5.989	
Inferior lobe of left lung	7	4.109± 5.689	
Upper lobe of right lung	10	7.327 ± 9.985	
Inferior lobe of right lung	13	10.590 ± 9.951	
Tumor size(cm)	40		0.8092
≥2cm	18	6.669±7.934	
<2cm	22	7.345±9.344	
T stage	40		0.3181
T1-2	32	6.350 ± 8.027	
T3-4	8	9.802 ± 10.919	
N stage	40		0.0258
N0	35	5.906 ± 7.299	
N1-2	5	14.988± 13.562	
TNM stage	40		0.0070
I	27	6.033 ± 7.592	
II	8	3.761± 5.849	
III	5	17.731 ± 11.015	
Hiopathological typing	40		0.0407
Acinar	22	4.857 ± 6.511	
Papillary	10	10.743± 9.863	
Micropapillary	4	1.067±0.515	
Mucoid	1	12.366±0.000	
Solid	3	16.903± 14.775	

N6-Methyladenosine (m6A) plays a vital role in the epigenetic regulation of the mammalian mRNAs since it was first identified in the 1970s (25). M6A has been shown by more and more evidences to participate in a variety of disease genesis and tumorigenesis, thus drawing a lot of concerns (26). Emerging theories show that the m6A modification could remarkably regulate the tumorigenesis of human cancers, which might provide a potential therapeutic target.

There are about 7600 mRNA transcripts that could be found in the m6A sites (27). The m6 A occurs mostly in RRACH consensus sequence, among which, the R might be G or A, while the H might be A, C or U (28-30). Based on current experimental studies, m6A decoration retains mRNA stability and mRNA splicing, followed by a chain-reaction on mRNA expression levels (31). Such an effect may arouse cancer cells expressions and biological activities, hence accelerating tumor progression. There are three types of m6A related proteins including writers, erasers and readers (32, 33). Among these key enzymes, RBM15 has been found to regulate a series of human cancers, such as acute megakaryoblast leukemia(34), colon Adenocarcinoma(35) and so on.

This study is aimed to explore the possible carcinogenic effects of RBM15 in LUAD, which led to the findings that RBM15 was significantly more up-regulated in the hospital LUAD patients than in the normal tissues, which was in accordance with the previous TCGA database literature reported. With the RBM15 function tested in the LUAD cell line, A549 and H1734 cells selected as cell models and the biological function of RBM15 in LUAD cells detected by proliferation, invasion and migration in vitro, the LUAD cell lines were screened by Western blot, thus constructing A549 and H1734 cell lines with interfering RBM15, and observing cell morphology, proliferation, migration, colony formation, and invasion capabilities after RBM15 gene downregulated expression. In CCK8 determination of cell proliferation experiments, RBM15 gene down-regulation of A549 and H1734 cells proliferation were significantly lower than those in the control group, indicating that RBM15 gene downregulated expression inhibited A549 and H1734 cells proliferation, which indicated that RBM15 is possibly involved in regulating the growth of LUAD cells. To further explore the relationship between RBM15 and tumor invasion, the results were verified by transwell and scratch experiments, showing that A549 and H1734 cell migration and invasion ability were impaired after the down-regulation of RBM15, leading to the conclusion that RBM15 had participated not only in the growth of LUAD cells but also in the migration and invasion of LUAD cells. In cell cycle testing, flow cytometry data demonstrated that down-regulation of RBM15 had increased the ratio of G0/G1 phase cells, and reduced the ratio of S, G2/M phase cells, indicating that downregulation of RBM15had blocked stage G0/G1 cells. Next, the result of verifying the relationship between down-regulation of RBM15group and m6A modification demonstrated that RBM15 had a positive correlation with m6A modification, that m6A modifications showed low expression by using RBM15 gene downregulation of A549 and H1734 cells, and that m6A modification effects include promoting cell proliferation, controlling apoptosis, and promoting the invasion and metastasis of cancer cells. Finally, in clinicopathologic studies, the expression level of RBM15 was found to be associated with LN metastasis, TNM stage, and histopathological typing, which was speculated to be providing a significant basis for clinical diagnosis.

In conclusion, RBM15 was confirmed to be overexpressed in LUAD and suppressing RBM15 expression could significantly inhibit the m6A methylation modification levels, thus inhibiting proliferation and promoting apoptosis, which leads to the speculation that RBM15 might be an oncogene in the process of LUAD occurring, suggesting the feasibility of using it as one of the biomarkers of LUAD.

Acknowledgments

Not applicable.

Author contribution

MSM put forward the idea and designed the research; WW performed the western blot analysis, RT qPCR assays and cell experiments; BYW and YCY performed the immunohistochemistry assays; YCH and GQZ performed SSPS data analysis; MSM wrote the manuscript; LHY revised the manuscript; All authors read and approved the final manuscript.

Funding

This work was supported by the National Natural Science Foundation of China (No.81860325) and the High-level health technical personnel of Yunnan Provincial Health Commission (No. L-2017006).

Interest Conflict

The authors declare no conflicts of interest.

References

1. Sung H, Ferlay J, Siegel R L, Laversanne M, Soerjomataram I, Jemal A, et al. Global Cancer Statistics 2020: GLOBOCAN Estimates of Incidence and Mortality Worldwide for 36 Cancers in 185 Countries. CA Cancer J Clin.2021; 71(3):209-49.
2. Olfati A and Moradi-kor N. The Therapeutic Effect of Statins on Survival of Patients with Gastrointestinal Cancer: a Review. International Journal of Advanced Biological and Biomedical Research.2019; 7(3):191-203.
3. Ahmadi Z, Ashrafizadeh M and Forouzan M. Apoptotic and autophagic modulation by nicotine. International Journal of Advanced Biological and Biomedical Research.2019; 7(3):263-73.
4. Deshotels L, Chaaya G and Komiya T. An Overview of Lung and Breast Cancer Using the National Cancer Database. Asian Pacific journal of cancer prevention: APJCP.2020; 21(1):163.
5. Siegel R L, Miller K D, Fuchs H E and Jemal A. Cancer Statistics, 2021. CA Cancer J Clin.2021; 71(1):7-33.
6. Network. C G A R a. Comprehensive molecular profiling of lung adenocarcinoma. Nature.2014; 511(7511):543-50.
7. Ahmadinejad M, Obeidavi Z, Aaliehpour A, Beiranvand B, Sheikhi E, Babaei M, et al. Human Cystic Echinococcosis in Lorestan province, Southwest Iran: A retrospective epidemiological study of surgical cases during a 10 years period (2005-2014). International Journal of Advanced Biological and Biomedical Research.2015; 3(4):320-5.
8. Fazeli-Nasab B, Sayyed R Z and Sobhanizadeh A. In Silico Molecular Docking Analysis of α-Pinene: An Antioxidant and Anticancer Drug Obtained from Myrtus communis. Int J Cancer Manag.2021; 14(2):e89116.
9. Kristina S A, Permitasari N P A L, Krisnadewi K I and Santosa K A. Incidence and mortality of cancers related to secondhand smoking in Southeast Asia countries. Asian Pacific Journal of Cancer Prevention: APJCP.2019; 20(3):971.
10. Zhang C, Fu J and Zhou Y. A Review in Research Progress Concerning m6A Methylation and Immunoregulation. Front Immunol.2019; 10(922.
11. Wu Y, Xie L, Wang M, Xiong Q, Guo Y, Liang Y, et al. Mettl3-mediated m(6)A RNA methylation regulates the fate of bone marrow mesenchymal stem cells and osteoporosis. Nat Commun.2018; 9(1):4772.
12. Abu-Duhier F, Javid J, Sughayer M, Mir R, Albalawi T and Alauddin M S. Clinical significance of circulatory miRNA-21 as an efficient non-invasive biomarker for the screening of lung cancer patients. Asian Pacific journal of cancer prevention: APJCP.2018; 19(9):2607.
13. Chen P, Wang B L, Pan B S and Guo W. MiR-1297 regulates the growth, migration and invasion of colorectal cancer cells by targeting cyclo-oxygenase-2. Asian Pac J Cancer Prev.2014; 15(21):9185-90.
14. Wu J, Qi X, Liu L, Hu X, Liu J, Yang J, et al. Emerging Epigenetic Regulation of Circular RNAs in Human Cancer. Mol Ther Nucleic Acids.2019; 16(589-96.
15. Zhao W, Ma X, Liu L, Chen Q, Liu Z, Zhang Z, et al. SNHG20: A vital lncRNA in multiple human cancers. J Cell Physiol.2019, 10.1002/jcp.28143
16. Khosravanian A, Moslehipour A and Ashrafian H. A review on bioimaging, biosensing, and drug delivery systems based on graphene quantum dots. Progress in Chemical and Biochemical Research.2021; 4(1):44-56.
17. Hatami A and Azizi Haghighat Z. Evaluation of Application of Drug Modeling in Treatment of Liver and Intestinal Cancer. Progress in Chemical and Biochemical Research.2020; 4(2):220-33.
18. Zare Kazemabadi F and Heydarinasab A. Using a two-Dimensional Finite Element Model to Simulate Biothermal Transfer in the Human Eye) by Considering the Rate of Tear Evaporation and Radiation to the Eye Surface. Progress in Chemical and Biochemical Research.4(3):305-18.
19. Zad Z R, Davarani S S H, Taheri A R and Bide Y. Highly selective determination of amitriptyline using Nafion-AuNPs@ branched polyethyleneimine-derived carbon hollow spheres

in pharmaceutical drugs and biological fluids. Biosensors and Bioelectronics.2016; 86(616-22.
20. Pendleton K E, Chen B, Liu K, Hunter O V, Xie Y, Tu B P, et al. The U6 snRNA m(6)A Methyltransferase METTL16 Regulates SAM Synthetase Intron Retention. Cell.2017; 169(5):824-35.e14.
21. Chen B, Li Y, Song R, Xue C and Xu F. Functions of RNA N6-methyladenosine modification in cancer progression. Mol Biol Rep.2019; 46(2):2567-75.
22. Lan Q, Liu P Y, Haase J, Bell J L, Hüttelmaier S and Liu T. The Critical Role of RNA m(6)A Methylation in Cancer. Cancer Res.2019; 79(7):1285-92.
23. Hu M, Yang Y, Ji Z and Luo J. RBM15 Functions in Blood Diseases. Curr Cancer Drug Targets.2016; 16(7):579-85.
24. Alarbeed I F, Wafa A, Moassass F, Al-Halabi B, Alachkar W and Aboukhamis I. Two Novel Mutations of the NPM1 Gene in Syrian Adult Patients with Acute Myeloid Leukemia and Normal Karyotype. Asian Pacific Journal of Cancer Prevention: APJCP.2021; 22(1):227.
25. Choe J, Lin S, Zhang W, Liu Q, Wang L, Ramirez-Moya J, et al. mRNA circularization by METTL3-eIF3h enhances translation and promotes oncogenesis. Nature.2018; 561(7724):556-60.
26. Mendel M, Chen K M, Homolka D, Gos P, Pandey R R, McCarthy A A, et al. Methylation of Structured RNA by the m(6)A Writer METTL16 Is Essential for Mouse Embryonic Development. Mol Cell.2018; 71(6):986-1000.e11.
27. Zhou J, Wang J, Hong B, Ma K, Xie H, Li L, et al. Gene signatures and prognostic values of m6A regulators in clear cell renal cell carcinoma - a retrospective study using TCGA database. Aging (Albany NY).2019; 11(6):1633-47.
28. Chen M, Wei L, Law C T, Tsang F H, Shen J, Cheng C L, et al. RNA N6-methyladenosine methyltransferase-like 3 promotes liver cancer progression through YTHDF2-dependent posttranscriptional silencing of SOCS2. Hepatology.2018; 67(6):2254-70.
29. Wu J, Zhao W, Wang Z, Xiang X, Zhang S and Liu L. Long non-coding RNA SNHG20 promotes the tumorigenesis of oral squamous cell carcinoma via targeting miR-197/LIN28 axis. J Cell Mol Med.2019; 23(1):680-8.
30. Yang F, Jin H, Que B, Chao Y, Zhang H, Ying X, et al. Dynamic m(6)A mRNA methylation reveals the role of METTL3-m(6)A-CDCP1 signaling axis in chemical carcinogenesis. Oncogene.2019; 38(24):4755-72.
31. Ding Y, Qi N, Wang K, Huang Y, Liao J, Wang H, et al. FTO Facilitates Lung Adenocarcinoma Cell Progression by Activating Cell Migration Through mRNA Demethylation. Onco Targets Ther.2020; 13(1461-70.
32. Deng X, Su R, Stanford S and Chen J. Critical Enzymatic Functions of FTO in Obesity and Cancer. Front Endocrinol (Lausanne).2018; 9(396.
33. Tong J, Flavell R A and Li H B. RNA m(6)A modification and its function in diseases. Front Med.2018; 12(4):481-9.
34. Langenberg-Ververgaert K, Renzi S, Fuligni F, Davidson S, Abdelhaleem M, Lo W, et al. TERT promotor variant associated with poor clinical outcome in a patient with novel RBM15-MKL1 fusion-positive pediatric acute megakaryoblastic leukemia. Pediatr Blood Cancer.2021; 68(1):e28542.
35. Liu T, Li C, Jin L, Li C and Wang L. The Prognostic Value of m6A RNA Methylation Regulators in Colon Adenocarcinoma. Med Sci Monit.2019; 25(9435-45.